Journal of Structural Biology 214 (2022) 107824

Contents lists available at ScienceDirect

Journal of Structural Biology

journal homepage: www.elsevier.com/locate/yjsbi

Disorder-to-order transition of Synaptobrevin-2: Tracing the conformational diversity of a synaptic SNARE protein

Julia Hesselbarth, Carla Schmidt *

Interdisciplinary Research Center HALOmem, Institute of Biochemistry and Biotechnology, Charles Tanford Protein Center, Martin Luther University Halle-Wittenberg, Halle, Germany

A B S T R A C T

Synaptobrevin-2 is one of the key players of neuronal exocytosis. Together with Syntaxin-1A and SNAP25, it forms the core membrane fusion machinery that is responsible for neurotransmitter release and, therefore, signal transmission between neurons. However, in the absence of interaction partners, Synaptobrevin-2 is largely unstructured and exhibits an inherent flexibility. In this graphical review, we provide an overview on the structural states of Synaptobrevin-2 in the absence and in the presence of interaction partners. For this, we first depict its natural habitat, namely the presynaptic nerve terminal, and gather biophysical properties that are likely responsible for its structural diversity. We then provide an overview on key findings describing the disorder-to-order transition of Synaptobrevin-2 from a mostly unstructured protein to a highly structured protein complex component.

1. Introduction

Signal transmission between neurons takes place at specifically designed contact sites called synapses. In general, synapses are composed of the presynaptic nerve terminal, the synaptic cleft and the postsynaptic side (Chua et al., 2010) (Fig. 1). The presynapse is the storage location for synaptic vesicles (Fig. 1, step **i**), which undergo a trafficking cycle resulting in exocytosis of the vesicles and release of neurotransmitters into the synaptic cleft (Südhof, 1995). To achieve this, synaptic vesicles are first loaded with specific neurotransmitters. Loaded vesicles then form a pool of readily releasable docked vesicles in the active zone, where they are activated in a process called 'priming' (Fig. 1, step **ii**). Upon Ca^{2+}-influx, the synaptic vesicle and presynaptic plasma membrane fuse, and neurotransmitters are released into the synaptic cleft (Fig. 1, step **iii**). The signal is passed on to the next neuron through neurotransmitter receptors in the postsynaptic membrane, which trigger signalling cascades in the postsynaptic side. After fusion of the two membranes, synaptic vesicles are recycled through different recycling pathways (Mori and Takamori, 2018).

Synaptic vesicles are densely packed with proteins that fulfil the various functional tasks required during the synaptic vesicle cycle (Takamori et al., 2006). These proteins include, for instance, the subunits of the vesicular proton pump ('V-ATPase'), specific neurotransmitter transporters, the Ca^{2+}-sensor Synaptotagmin-1 or trafficking proteins such as the Rabs. In addition, there is a subset of typical synaptic vesicle proteins with less-understood function; examples are Synapsin, Synaptophysin/Synaptoporin, Synaptogyrin, CSP or SV2A/B. The major protein component of synaptic vesicles is Synaptobrevin-2 with approx. 70 copies per vesicle (Takamori et al., 2006). Synaptobrevin-2 belongs to the 'soluble N-ethylmaleimide-sensitive-factor attachment receptor' (SNARE) protein family and, together with Syntaxin-1A and SNAP25, constitutes the core membrane fusion machinery. Due to its inherent flexibility, Synaptobrevin-2 was found to interact, specifically and unspecifically, with many proteins of unstimulated synaptic vesicles (Wittig et al., 2021) (Fig. 1, panel **i**).

After vesicle priming (Fig. 1, panel **ii**), the vesicular and presynaptic membranes are in close proximity enabling spontaneous formation of the ternary SNARE complex upon intracellular Ca^{2+}-influx. For this, the mostly unstructured SNAREs, i.e. the vesicle protein Synaptobrevin-2 as well as Syntaxin-1A and SNAP25, which are both anchored to the presynaptic plasma membrane, assemble into a tightly packed four-helix bundle (Söllner et al., 1993; Sutton et al., 1998) (Fig. 1, panel **i**). Synaptobrevin-2 and Syntaxin-1A both contribute one alpha-helix, while SNAP25 contributes two alpha-helices to the SNARE complex. Helix zippering proceeds from the N- to the C-terminus of the proteins along their conserved SNARE motifs (Jahn and Scheller, 2006). Helix zippering of the natively unstructured SNAREs is assumed to overcome the energy required for membrane fusion (Gao et al., 2012).

In the absence of interaction partners, Synaptobrevin-2 is mostly unstructured. Several studies targeted its disorder-to-order transition from a natively unstructured protein to the highly structured component of the helical SNARE complex. These studies employed various

* Corresponding author.
E-mail address: carla.schmidt@biochemtech.uni-halle.de (C. Schmidt).

https://doi.org/10.1016/j.jsb.2021.107824
Received 30 September 2021; Received in revised form 17 November 2021; Accepted 6 December 2021
Available online 10 December 2021

Synaptobrevin-2 fragments including, for instance, the full-length protein, the soluble domain or the transmembrane domain (TMD) (Fig. 2**A**). The full-length protein is characterized by (i) a 94 residues-long cytosolic domain including the highly conserved SNARE motif (residues 31–85) and the dynamic juxtamembrane domain (JMD, residue 86–94), (ii) a TMD (residues 95–114) anchoring the protein to the vesicular membrane as well as (iii) a short lumenal domain of only 2 residues (residues 115/116) (Fig. 2**A**). The flexibility of Synaptobrevin-2 is visualized by its AlphaFold score revealing, with high confidence, a C-terminal transmembrane helix which extends to the juxtamembrane linker and the C-terminal part of the SNARE motif (Jumper et al., 2021). This confidence measure continuously decreases towards the N-terminus of the protein predicting a completely disordered N-terminus (Fig. 2**A**). The AlphaFold prediction correlates well with the conservation of amino acid residues among Synaptobrevin-2 homologues (Ashkenazy et al., 2016); the C-terminal half of the protein, i.e. the TMD, the JMD and the C-terminal SNARE motif, are conserved between 150 Synaptobrevin-2 homologues while the flexible N-terminus is less conserved (Fig. 2**B**). Interestingly, several cleavage sites of Botulinum and Tetanus neurotoxins are located in the conserved region indicating the importance of this region for exocytosis and allowing neurotoxins to target different species (Montecucco and Schiavo, 1995) (Fig. 2**C**). Plotting hydrophobicity and charge of Synaptobrevin-2, confirms the presence of a C-terminal, hydrophobic TMD. Importantly, the JMD exhibits a comparably high positive charge responsible for interactions with negatively charged phospholipids (Williams et al., 2009) (Fig. 2**D** and **E**).

The conformational diversity of Synaptobrevin-2 in the absence of interaction partners ranges from a completely disordered protein over partially folded states to a fully structured complex component (Sutton et al., 1998; Fasshauer et al., 1997; Hazzard et al., 1999). Similarly, different oligomeric states including monomers, dimers of the TMD as well as oligomers formed between the soluble domain or even unspecifically were reported (Margittai et al., 2001; Laage and Langosch, 1997; Wittig et al., 2019) (Fig. 3**A**). In the presence of DPC micelles, partial folding of the full-length protein was observed including the predicted TMD ('helix III') as well as extension of the transmembrane helix towards the JMD and the C-terminal SNARE motif ('helix II') and an additional helix including parts of the SNARE motif ('helix I'). Notably, these structural features were highly dynamic accounting for a broad conformational space (Ellena et al., 2009) (Fig. 3**B**). Formation of 'helix II' and 'helix III' (see above) was also observed in nanodiscs and liposomes, however, the remaining protein was found to be disordered in lipid bilayers (Brewer et al., 2011) (Fig. 3**C**). These observations were supported by a study comparing formation of helical elements in different lipid environments; the SNARE motif of Synaptobrevin-2 was found to be sensitive towards membrane curvature, and the helical and random coil states are best described by an equilibrium between

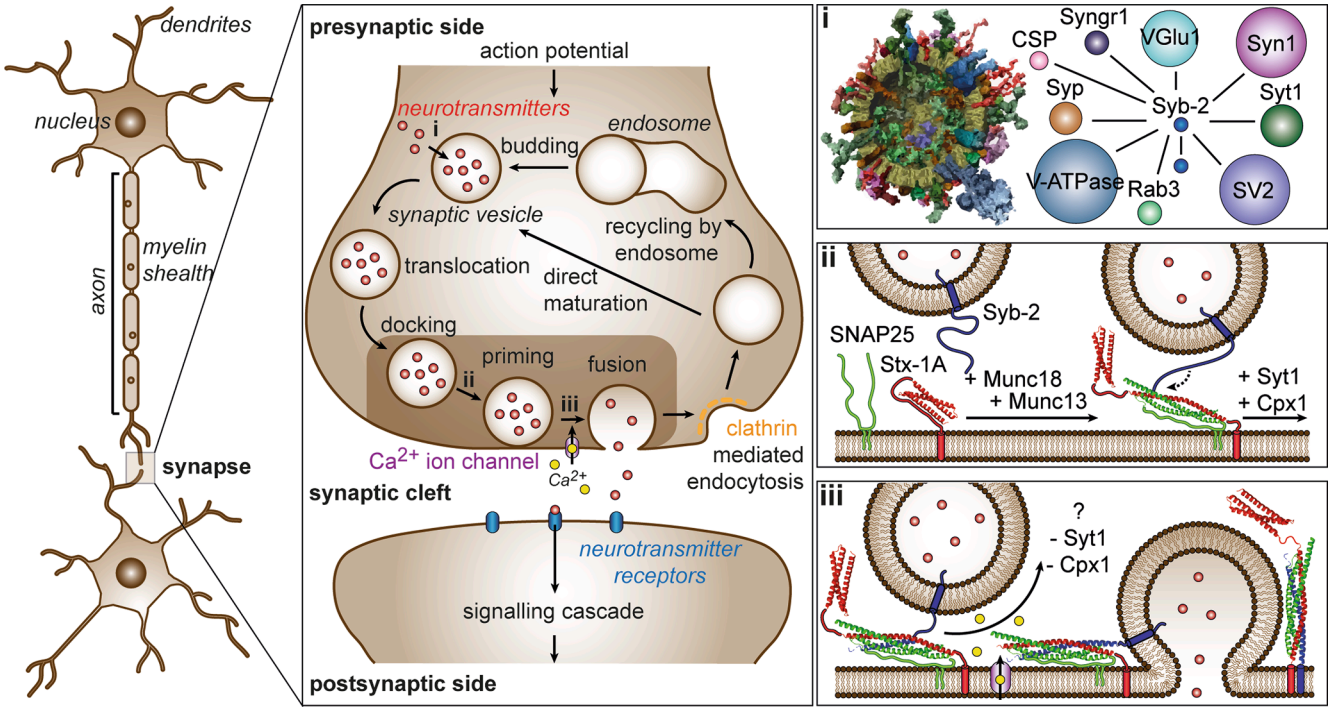

Fig. 1. Signal transmission between neurons is mediated by SNARE complex assembly. Neurons interact through special interaction sites, called synapses, that are formed between the axon of the first neuron and a dendrite of the second neuron (lhs). In the cytosol of the presynapse, synaptic vesicles are first loaded with neurotransmitters (step i) and then migrate to the 'active zone' (brown shading), where they dock at the presynaptic membrane and are activated by SNARE complex assembly (step ii). Upon Ca^{2+}-influx, fusion of the two membranes proceeds, resulting in neurotransmitter release into the synaptic cleft (step iii). Diffusion of neurotransmitters to the postsynaptic terminal forwards the action potential by initiating a signalling cascade. Clathrin-mediated endocytosis regenerates the vesicles directly by loading with neurotransmitters or by budding from the endosome (Chua et al., 2010; Südhof, 1995) (middle panel). (**i**) Synaptic vesicles are storage organelles of neurotransmitters densely packed with proteins. These include many copies of Synaptobrevin-2 (Syb-2) as well as other vesicular proteins such as the V-ATPase, Rab3, SV2, Synaptotagmin-1 (Syt1), Synapsin-1 (Syn1), Glutamat-transporter 1 (VGlu1), Synaptogyrin-1 (Syngr1), CSP and Synaptophysin (Syp) (Takamori et al., 2006). These proteins constitute an interaction network with Syb-2 as revealed by chemical cross-linking (Wittig et al., 2021). (Image of synaptic vesicle reprinted with permission from RightsLink.) (**ii**) In the absence of other SNAREs, vesicular Syb-2 (blue) and SNAP25 (green), which is bound to the plasma membrane, are unstructured. Munc18 keeps Syntaxin-1A (Stx-1A, red) in a 'closed' conformation. Recruitment of Munc13 then converts Stx-1A to an 'open' conformation enabling binding of SNAP25 and formation of the 'acceptor' complex that provides a binding site for Syb-2. SNARE assembly takes place from the N- towards the C-terminus and is regulated by Syt1 and Complexin-1 (Cpx1); the formed trans-SNARE complexes constitute activated intermediate states ('primed' synaptic vesicles) (Jahn and Scheller, 2006). (**iii**) In response to Ca^{2+}-influx (yellow), SNARE assembly is regulated by Syt1 and Cpx1 and proceeds following a largely unknown mechanism. As a result, the two membranes fuse, neurotransmitters are released and the final state during SNARE assembly, the cis-SNARE complex, is formed (Jahn and Scheller, 2006).

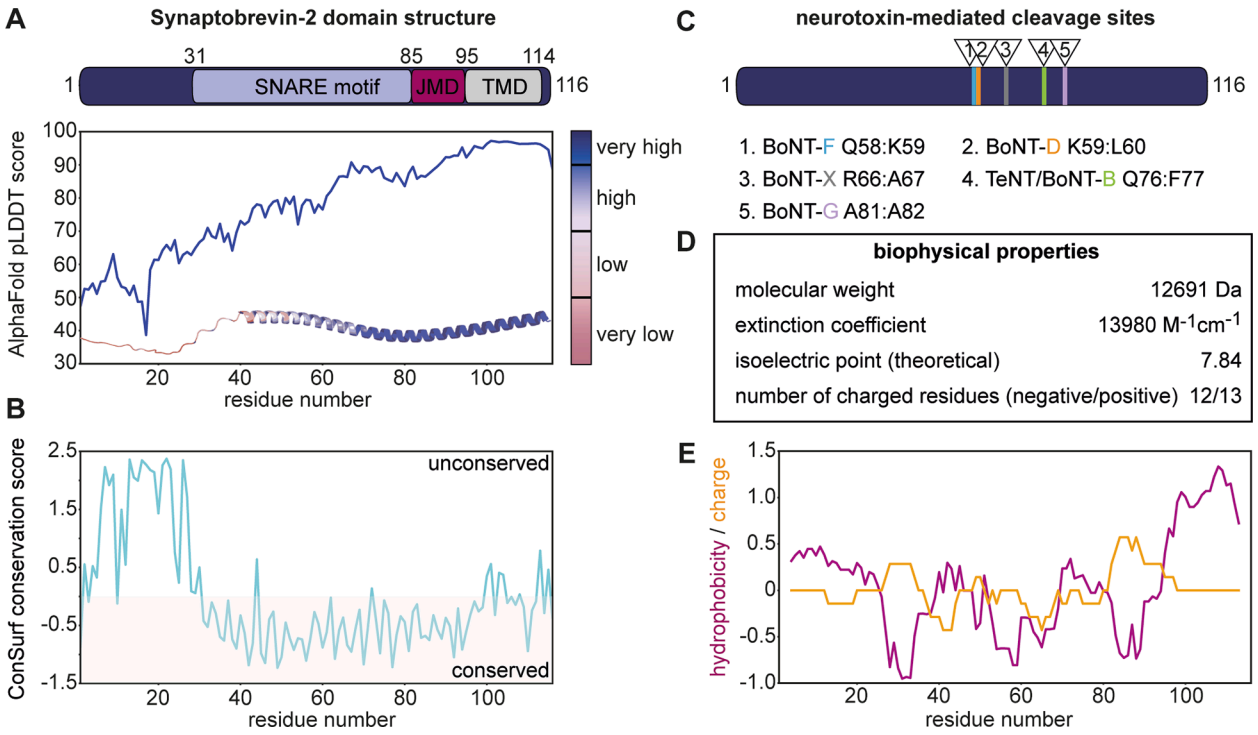

Fig. 2. Characterization of Synaptobrevin-2. Synaptobrevin-2 from *rattus norvegicus* (P63045) is a commonly used variant and is therefore explained as an example. (**A**) Synaptobrevin-2 domain structure and AlphaFold structure prediction (Jumper et al., 2021). The SNARE motif (light blue), the JMD (ruby) and the TMD (grey) are highlighted. The pLDDT per-residue confidence score (<50, very low; 50–70, low; 70–90, confident; >90, very high) of Synaptobrevin-2 is plotted against the residue number. The predicted structure reveals a disordered N-terminus and an increasing confidence for helical structures towards the C-terminus. (**B**) The ConSurf conservation score predicted from 150 aligned Synaptobrevin-2 homologues is plotted against the residue number (Ashkenazy et al., 2016). The SNARE motif and the JMD are highly conserved. (**C**) Location of Botulinum and Tetanus neurotoxin cleavage sites in Synaptobrevin-2 (Montecucco and Schiavo, 1995). (**D**) General biophysical properties based on the amino acid composition calculated by ExPASy (ProtParam) (Wilkins et al., 1999). (**E**) Hydrophobicity and charge plots. Hydrophobicity values for the residues based on Eisenberg were used (Eisenberg et al., 1984). Charges were defined as follows: Arg/Lys: +1; His: +0.5; Glu/Asp: −1 (EMBOSS charge). The mean hydrophobicity and charge scores were calculated using a rolling seven-residue window and plotted against the residue number.

unstructured and structured elements in the different environments (Liang et al., 2014).

Recently, transient lipid binding of Synaptobrevin-2 reconstituted in liposomes was analysed by NMR and fluorescence spectroscopy (Lakomek et al., 2019). In agreement with the structural characteristics of Synaptobrevin-2 (see above, Fig. 2), flexibility was found to decrease from the protein's N- to the C-terminus while lipid binding increases towards the C-terminus (Fig. 3**D**). Lipid binding in the JMD is likely caused by attraction of positively charged amino acids. Importantly, negatively charged amino acid residues located N-terminal of arginine 56 induce repulsion between the protein and the membrane making this residue a critical point in the amino acid sequence (Williams et al., 2009; Brewer et al., 2011; Lakomek et al., 2019). Electrostatic interactions between the JMD of Synaptobrevin-2 and Syntaxin-1A were further hypothesized to induce membrane bending (Williams et al., 2009). This effect supposedly contributes to pulling the synaptic vesicle and the presynaptic membranes together, thereby, facilitating membrane fusion during exocytosis of neurotransmitters. Two tryptophan residues are supporting membrane interactions in this model. A key residue in the TMD, namely glycine 100, induces a kink in the helix ensuring certain flexibility of the assembled complex (Han et al., 2016) (Fig. 3**E**). Finally, interaction of Synaptobrevin-2 with Syntaxin-1A and SNAP25 results in formation of the SNARE complex (Sutton et al., 1998; Stein et al., 2009). In this complex, the helices of the four helix bundle extend into the lipid membrane resulting in reduced flexibility of the protein assembly (Stein et al., 2009). The SNARE motifs of Synaptobrevin-2, Syntaxin-1A and SNAP25 form 15 layers of hydrophobic amino acid residues as well as one ionic layer in the middle of the SNARE assembly (Fig. 3**F**) (Sutton et al., 1998; Ossig et al., 2000). After successful membrane fusion, the SNARE complex is disassembled by the NSF/α-SNAP degradation machinery and, thereby, prepared for a new round of exocytosis (Südhof, 1995; Jahn and Scheller, 2006).

In summary, the conformational diversity of Synaptobrevin-2, in the absence or presence of interaction partners, was targeted by a range of complementary structural biology techniques. While NMR is generally well-suited to visualise conformational dynamics of proteins, the complexity of the target system is often limited and, therefore, most studies focussed on the individual protein. EPR and fluorescence spectroscopy, on the other hand, provided information on interactions of Synaptobrevin-2 with other SNARE proteins as well as on changes in the environment of specifically labelled amino acid residues; however, these techniques required site-directed point mutations of the protein(s) and selection of the labelled residues was critical for the outcome of the experiments. X-ray crystallography delivered high-resolution structures of the SNARE complex reflecting snapshots of the dynamic ensemble. While the different techniques have their advantages and disadvantages, it became apparent that a combination of complementary approaches was most powerful to uncover the dynamic states of Synaptobrevin-2 in different (lipid) environments. Depending on the research question, the target system had to be adjusted and simplified. In addition to experimental studies, computational approaches likely gain importance in future studies; they are, in theory, applicable to any system of unlimited complexity and modifications of the protein structures/sequences are not required.

Declaration of Competing Interest

The authors declare that they have no known competing financial

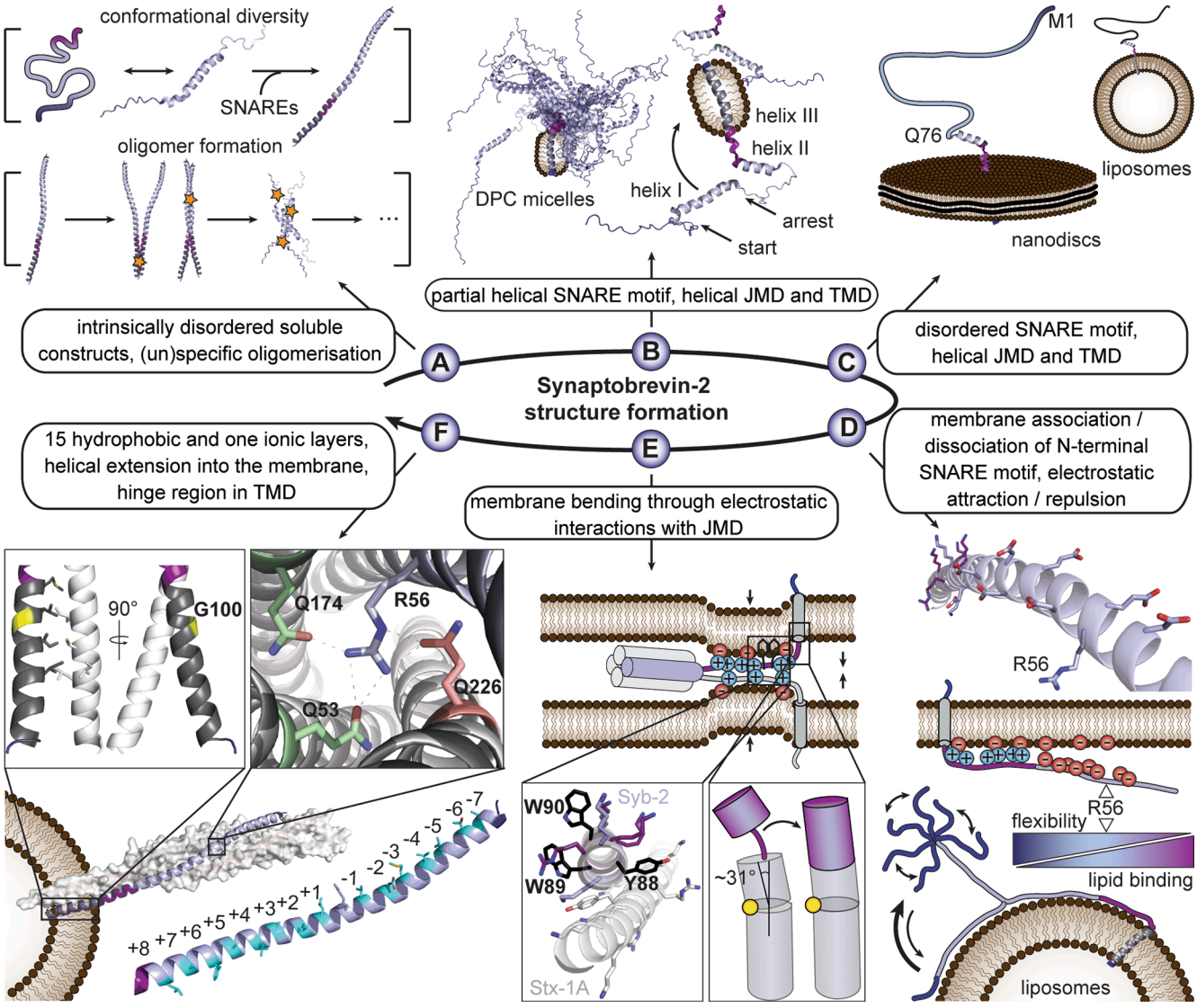

(caption on next page)

Fig. 3. Structural changes of Synaptobrevin-2 in the absence and presence of interaction partners. (**A**) CD, NMR and EPR spectroscopy revealed disorder of the cytosolic domain of Synaptobrevin-2 including partial helical structures (Fasshauer et al., 1997; Hazzard et al., 1999; Margittai et al., 2001). Interactions with other SNAREs result in helix formation (Sutton et al., 1998; Stein et al., 2009). Dimers and higher oligomers were identified by chemical cross-linking of the TMD (Laage and Langosch, 1997) as well as cytosolic variants of Synaptobrevin-2 (Wittig et al., 2019). Native MS further revealed additive oligomerisation in an 'aggregation like' manner (Wittig et al., 2019). (**B**) The presence of DPC micelles induces formation of helical structures resulting in 'helix I' (residues 36–54) and 'helix II' (residues 77–88), as well as in 'helix III' (residues 93–115) when the full-length construct is employed (PDB-ID: 2KOG) (Ellena et al., 2009). Helices I and II are separated by the natively disordered C-terminal SNARE motif, adjacent to the highly dynamic N-terminus resulting in high flexibility of the structural elements. The amphipathic helix I, therefore, interacts with the micelle surface in many different orientations. Formation of helix I is assumed to be energetically favoured functioning as a 'nucleation' site for rapid SNARE helix zippering starting from the N-terminus and being transiently stopped at the disordered C-terminal SNARE motif until regulatory proteins restart the assembly (Ellena et al., 2009). (**C**) NMR analysis of Synaptobrevin-2 in nanodiscs and liposomes revealed helical structures of the TMD and JMD induced by a cluster of basic residues. Additional helical structures or lipid binding were not observed. On the contrary, the disordered SNARE motif was found to be reluctant towards lipid membranes independent of the lipid composition (Brewer et al., 2011). (**D**) The crystal structure of Synaptobrevin-2 (PDB-ID: 3HD7) highlighting charged residues of the JMD and C-terminal SNARE motif (blue, positively charged; red, negatively charged), as well as a cartoon visualising membrane attraction of the positively charged linker and membrane repulsion of the negatively charged C-terminal SNARE motif are shown (Williams et al., 2009; Brewer et al., 2011; Lakomek et al., 2019). NMR and fluorescence spectroscopy further revealed general intrinsic disorder of Synaptobrevin-2 reconstituted in liposomes with decreasing flexibility from the N- towards the C-terminus including a local maximum of rigidity at the central arginine 56 and increasing lipid binding affinity in the opposite direction. An equilibrium of a membrane-bound conformation with low binding affinity and a dissociated conformation of the N-terminal SNARE motif with the highly flexible N-terminus was proposed (Lakomek et al., 2019). (**E**) A cartoon visualising the interactions of Synaptobrevin-2 with the other SNAREs in early SNARE assembly stages is shown. Positively charged linker regions of Synaptobrevin-2 and Syntaxin-1A create a local positive potential interacting with negatively charged lipids, thereby, inducing protrusion of the membrane and repositioning of the preassembled SNARE complex in close proximity of the membrane (Williams et al., 2009). Tryptophan residues of the aromatic motif (Y88, W89, W90) of Synaptobrevin-2, highlighted in the crystal structure (black, PDB-ID: 3HD7), insert into the lipid membrane (Williams et al., 2009). The dynamics of the TMD (grey) resulting from the aromatic residues at the membrane surface and a central hinge formed by glycine 100 (yellow, ball representation) influence the conformation of the linker. The TMD was shown to be present in a tilted (~31°) conformation with partially folded JMD and a less bent conformation (Han et al., 2016). (**F**) Synaptobrevin-2 (blue cartoon) bound to the interaction site formed by SNAP25 and Syntaxin-1A (white, surface representation) resulting in the four-helical bundle of the SNARE core complex; helical structures extend into the lipid membrane (PDB-ID: 3HD7) (Stein et al., 2009). Stability of this assembly is accomplished by formation of 15 parallel hydrophobic layers (cyan) and one central ionic layer, the zero-layer, composed of three glutamines (Q53, Q174, Q226) and the central arginine 56 of Synaptobrevin-2 (Sutton et al., 1998; Stein et al., 2009). Interactions between Synaptobrevin-2 and Syntaxin-1A further form a basic-aromatic layer within the linker region (Stein et al., 2009). Amino acid residues within the ionic and the aromatic layers are crucial for SNARE complex stability as revealed by mutational analysis (Stein et al., 2009; Ossig et al., 2000). The TMDs interact at their N-termini; amino acid residues of the interaction interface are shown as sticks. On the contrary, the TMDs are separated at their C-termini indicating conformational flexibility resulting from the central glycine 100, which functions as flexible hinge (yellow) (Han et al., 2016).

interests or personal relationships that could have appeared to influence the work reported in this paper.

Acknowledgements

We thank Julian Bender for help with generating the plots shown in Fig. 2 and Tommy Hofmann for comments on the manuscript. We acknowledge funding from the Deutsche Forschungsgemeinschaft (DFG, German Research Foundation, project number 391498659, RTG 2467 "Intrinsically Disordered Proteins – Molecular Principles, Cellular Functions, and Diseases"), the Federal Ministry for Education and Research (BMBF, ZIK programme, 03Z22HN22), the European Regional Development Funds (EFRE, ZS/2016/04/78115) and the MLU Halle-Wittenberg.

References

Ashkenazy, H., Abadi, S., Martz, E., Chay, O., Mayrose, I., Pupko, T., Ben-Tal, N., 2016. ConSurf 2016: an improved methodology to estimate and visualize evolutionary conservation in macromolecules. Nucleic Acids Res. 44 (W1), W344–W350.

Brewer, K.D., Li, W., Horne, B.E., Rizo, J., 2011. Reluctance to membrane binding enables accessibility of the synaptobrevin SNARE motif for SNARE complex formation. Proc. Natl. Acad. Sci. 108 (31), 12723–12728.

Chua, J.J.E., Kindler, S., Boyken, J., Jahn, R., 2010. The architecture of an excitatory synapse. J. Cell Sci. 123 (6), 819–823.

Eisenberg, D., Schwarz, E., Komaromy, M., Wall, R., 1984. Analysis of membrane and surface protein sequences with the hydrophobic moment plot. J. Mol. Biol. 179 (1), 125–142.

Ellena, J.F., Liang, B., Wiktor, M., Stein, A., Cafiso, D.S., Jahn, R., Tamm, L.K., 2009. Dynamic structure of lipid-bound synaptobrevin suggests a nucleation-propagation mechanism for trans-SNARE complex formation. Proceedings of the National Academy of Sciences of the United States of America 106.

Fasshauer, D., Otto, H., Eliason, W.K., Jahn, R., Brünger, A.T., 1997. Structural changes are associated with soluble n-ethylmaleimide-sensitive fusion protein attachment protein receptor complex formation*. J. Biol. Chem. 272 (44), 28036–28041.

Gao, Y., Zorman, S., Gundersen, G., Xi, Z., Ma, L.u., Sirinakis, G., Rothman, J.E., Zhang, Y., 2012. Single reconstituted neuronal SNARE complexes zipper in three distinct stages. Science 337 (6100), 1340–1343.

Han, J., Pluhackova, K., Bruns, D., Böckmann, R.A., 2016. Synaptobrevin transmembrane domain determines the structure and dynamics of the SNARE motif and the linker region. Biochimica et Biophysica Acta (BBA) - Biomembranes 1858 (4), 855–865.

Hazzard, J., Südhof, T.C., Rizo, J., 1999. NMR analysis of the structure of synaptobrevin and of its interaction with syntaxin. J. Biomol. NMR 14, 203–207.

Jahn, R., Scheller, R.H., 2006. SNAREs–engines for membrane fusion. Nature reviews. Mol. Cell Biol. 7 (9), 631–643.

Jumper, J., Evans, R., Pritzel, A., Green, T., Figurnov, M., Ronneberger, O., Tunyasuvunakool, K., Bates, R., Žídek, A., Potapenko, A., Bridgland, A., Meyer, C., Kohl, S.A.A., Ballard, A.J., Cowie, A., Romera-Paredes, B., Nikolov, S., Jain, R., Adler, J., Back, T., Petersen, S., Reiman, D., Clancy, E., Zielinski, M., Steinegger, M., Pacholska, M., Berghammer, T., Bodenstein, S., Silver, D., Vinyals, O., Senior, A.W., Kavukcuoglu, K., Kohli, P., Hassabis, D., 2021. Highly accurate protein structure prediction with AlphaFold. Nature 596 (7873), 583–589.

Laage, R., Langosch, D., 1997. Dimerization of the synaptic vesicle protein synaptobrevin (vesicle-associated membrane protein) II depends on specific residues within the transmembrane segment. Eur. J. Biochem. 249 (2), 540–546.

Lakomek, N.-A., Yavuz, H., Jahn, R., Pérez-Lara, Á., 2019. Structural dynamics and transient lipid binding of synaptobrevin-2 tune SNARE assembly and membrane fusion. Proc. Natl. Acad. Sci. USA 116 (18), 8699–8708.

Liang, B., Dawidowski, D., Ellena, J.F., Tamm, L.K., Cafiso, D.S., 2014. The SNARE motif of synaptobrevin exhibits an aqueous-interfacial partitioning that is modulated by membrane curvature. Biochemistry 53 (9), 1485–1494.

Margittai, M., Fasshauer, D., Pabst, S., Jahn, R., Langen, R., 2001. Homo- and heterooligomeric SNARE complexes studied by site-directed spin labeling. J. Biol. Chem. 276 (16), 13169–13177.

Montecucco, C., Schiavo, G., 1995. Structure and function of tetanus and botulinum neurotoxins. Quart. Rev. Biophys. 28 (4), 423–472.

Mori, Y., Takamori, S., 2018. Molecular signatures underlying synaptic vesicle cargo retrieval. Front. Cell. Neurosci. 11.

R. Ossig, H.D. Schmitt, G.B. de, D. Riedel, S. Keränen, H. Ronne, H. Grubmüller, R. Jahn, Exocytosis requires asymmetry in the central layer of the SNARE complex, The EMBO Journal 19 (2000).

Söllner, T., Whiteheart, S.W., Brunner, M., Erdjument-Bromage, H., Geromanos, S., Tempst, P., Rothman, J.E., 1993. SNAP receptors implicated in vesicle targeting and fusion. Nature 362 (6418), 318–324.

Stein, A., Weber, G., Wahl, M.C., Jahn, R., 2009. Helical extension of the neuronal SNARE complex into the membrane. Nature 460 (7254), 525–528.
Südhof, T.C., 1995. The synaptic vesicle cycle: a cascade of protein-protein interactions. Nature 375 (6533), 645–653.
Sutton, R.B., Fasshauer, D., Jahn, R., Brunger, A.T., 1998. Crystal structure of a SNARE complex involved in synaptic exocytosis at 2.4 A resolution. Nature 395.
Takamori, S., Holt, M., Stenius, K., Lemke, E.A., Grønborg, M., Riedel, D., Urlaub, H., Schenck, S., Brügger, B., Ringler, P., Müller, S.A., Rammner, B., Gräter, F., Hub, J.S., De Groot, B.L., Mieskes, G., Moriyama, Y., Klingauf, J., Grubmüller, H., Heuser, J., Wieland, F., Jahn, R., 2006. Molecular anatomy of a trafficking organelle. Cell 127 (4), 831–846.
Wilkins, E., Gasteiger, A., Bairoch, J.C., Sanchez, K.L., Williams, R.D., Appel, D.F.H., 1999. Protein identification and analysis tools in the ExPASy server. Methods Mol. Biol. (Clifton N.J.) 112.
Williams, D., Vicôgne, J., Zaitseva, I., McLaughlin, S., Pessin, J.E., Martin, T.F.J., 2009. Evidence that electrostatic interactions between vesicle-associated membrane protein 2 and acidic phospholipids may modulate the fusion of transport vesicles with the plasma membrane. Mol. Biol. Cell 20 (23), 4910–4919.
Wittig, S., Haupt, C., Hoffmann, W., Kostmann, S., Pagel, K., Schmidt, C., 2019. Oligomerisation of synaptobrevin-2 studied by native mass spectrometry and chemical cross-linking. J. Am. Soc. Mass Spectrom. 30 (1), 149–160.
Wittig, S., Ganzella, M., Barth, M., Kostmann, S., Riedel, D., Pérez-Lara, Á., Jahn, R., Schmidt, C., 2021. Cross-linking mass spectrometry uncovers protein interactions and functional assemblies in synaptic vesicle membranes. Nat. Commun. 12 (1) https://doi.org/10.1038/s41467-021-21102-w.